NJC
Letter

Promoted phase transition of titania nanoparticles prepared by a photo-assisted sol-gel method

Haimei Liu, Wensheng Yang, Ying Ma, Yaan Cao and Jiannian Yao*†

Center for Molecular Science, Institute of Chemistry, The Chinese Academy of Sciences, Beijing 100080, P. R. China

Received (in Montpellier, France) 26th February 2002, Accepted 25th April 2002
First published as an Advance Article on the web 25th June 2002

A simple and efficient methodology, in which ultraviolet irradiation was introduced into the preparation of the titania colloids, has been established for the synthesis of phase-pure anatase with a grain size of about 3.6 nm at calcination temperatures as low as 100 °C. The XRD and Raman results indicate that the phase transition of TiO_2 from amorphous to anatase is promoted by UV light irradiation. It is also documented that the promoted formation of anatase upon calcination is due to the oxygen vacancy defects induced by photo-irradiation of the colloid during the sol-gel process.

Titanium dioxide has been studied extensively due to its high photocatalytic activity.[1,2] Among the three polymorphs of titania (rutile, anatase and brookite), anatase has a higher photoactivity than that of brookite or rutile.[3,4] An anatase powder with a high degree of crystallinity and small grain size is desirable to improve the photocatalytic activity.[5] Among the methods available for the synthesis of small TiO_2 particles, that is nanoparticles, the sol-gel method has been widely employed due to the inexpensive equipment required and the homogeneous and highly pure product produced. Usually, the particles obtained by this method are amorphous in nature and calcination temperatures higher than 350 °C are required to realize the transition from the amorphous material to the anatase phase.[6] However such high calcination temperatures will result in increased size of the nanoparticles. To obtain anatase TiO_2 with a small grain size, less than 5 nm, a reasonable pathway would be to lower the temperature of the phase transition. We have found that TiO_2 nanocrystals with high photocatalytic activity can be obtained at low calcination temperatures by using a photo-assisted sol-gel method.[7] In this work, we investigate in detail the phase transition behavior of TiO_2 nanoparticles prepared by this photo-assisted sol-gel method.

Fig. 1 shows the XRD patterns of TiO_2 powder samples, as-prepared and calcined at various temperatures. It can be seen that the sample calcined at 100 °C shows distinctive peaks at the d (nm) values of {101}(0.3528), {004}(0.2380), {200}(0.1896) and {204}(0.1482) [JCPDS Pattern No.21-1272 (TiO_2)], indicating that anatase has been formed at this temperature. As the temperature is increased, progressive increases in peak intensity accompanied by a sharpening of the peaks are observed, implying an increase in crystallinity of the anatase phase with increased temperature. After annealing at 400 °C, all peaks become sharper and narrower, which is indicative of crystal growth. The d (nm) values of the peaks are determined to be {101}(0.3517), {004}(0.2383), {200}(0.1894), {105}(0.1701), {211}(0.1665), {204}(0.1482), {116}(0.1365), {220}(0.1339), and {215} (0.1261), showing a decrease of the d values compared with those of the sample annealed at 100 °C. The insert shows the XRD pattern of a non-irradiated sample annealed at 100 °C. It is clearly seen that the sample dose not exhibit any peaks that can be attributed to anatase, which demonstrates that the sample remained amorphous in nature. This suggests that the photo-illumination applied during the sol-gel process can promote the phase transition and crystallinity of the TiO_2. Table 1 gives further details of the particle sizes, calculated by using the Scherrer equation [$L = 0.9\lambda/B(2\theta)\cos\theta$, where L is the crystallite size and $B(2\theta)$ is the full width at half-maximum (FWHM)], and specific surface areas of the particles calcined at different temperatures. It can be determined that the grain size of anatase particles is about 3.6 nm and the BET surface value is 239 $m^2\ g^{-1}$ when the calcination temperature is 100 °C. With increasing calcination temperature, the particle size increases and the specific surface area of the samples decreases.

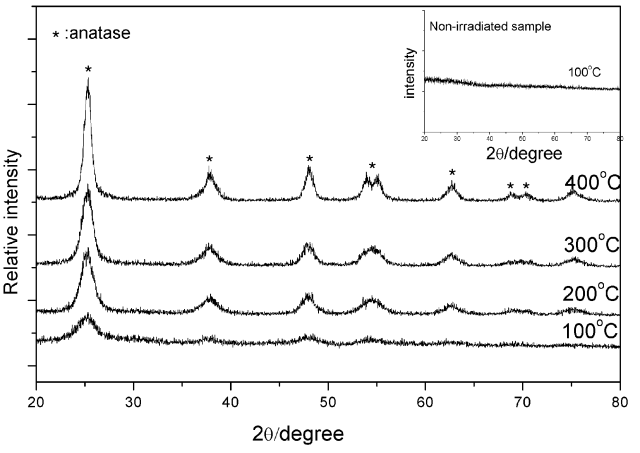

Fig. 1 X-Ray diffraction patterns of the powder samples, as-prepared and annealed at different temperatures. The insert shows the XRD pattern of a non-irradiated 100 °C sample.

Table 1 The main grain size and specific surface area of TiO_2 at various calcination temperatures

T/°C	Grain size[a] /nm	$S_{BET}/m^2\ g^{-1}$
100	3.6	239
200	6.0	204
300	7.1	198
400	12.7	158

[a] The data calculated from Fig. 1 are based on the Scherrer formula.

† Current address: Technical Institute of Physics and Chemistry, The Chinese Academy of Sciences, Beijing 100101, P. R. China Tel: +86-10-6488-8154; fax: +86-10-6487-9375; e-mail: jnyao@ipc.ac.cn

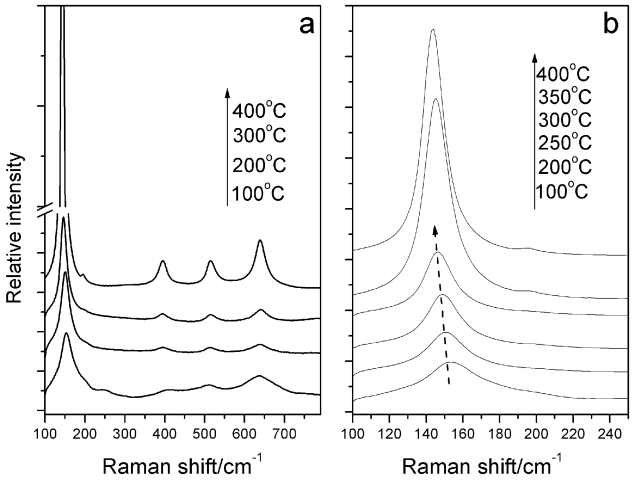

Fig. 2 Raman spectra of the powder samples (a) and the amplified spectra (b) in the region of 100–250 cm^{-1}, which show the peak shift with increasing temperatures.

Fig. 2 shows the Raman spectra of TiO_2 powders calcined at different temperatures. For the four samples calcined at 100, 200, 300 and 400 °C, the observed characteristic bands at 638, 513 and 393 cm^{-1} [Fig. 2(a)], assigned to the E_g, $(A_{1g} + B_{1g})$ and B_{1g} vibrational modes, respectively, indicate the presence of the anatase phase in all four samples.[8,9] However, the strongest E_g vibration band experiences a shift from 144.6 to 153.6 cm^{-1} as the calcination temperature decreases from 400 to 100 °C. Such a shift suggests that the ratios of Ti and O in the two samples annealed at 100 and 200 °C are nonstoichiometric. The formula can be calculated to be $TiO_{<1.88}$ and $TiO_{<1.97}$, respectively, by the peak positions of 153.6 cm^{-1} (annealed at 100 °C) and 151.2 cm^{-1} (annealed at 200 °C),[10,11] indicating the existence of oxygen defects in these two samples[12,13] ([Fig. 2(b)]. For the samples annealed at 300 and 400 °C, the strongest band appears at 144.6 cm^{-1}, meaning that the stoichiometric ratio of anatase TiO_2 has been recovered after the high temperature annealing in air. However, as for the non-irradiated samples annealed at 100 and 200 °C, the Raman spectra do not show any characteristic bands of anatase (not shown). This also confirms that UV irradiation can promote the phase transition of the TiO_2 particles.

The existence of oxygen defects in UV-irradiated samples was further investigated by X-ray photoelectron spectroscopy (XPS). Fig. 3 shows the Ti2p and O1s core level XPS spectra of the sample calcined at 100 °C. The two peaks located at 458.7 and 464.5 eV can be assigned to the core levels of $Ti^{4+}2p_{3/2}$ and $Ti^{4+}2p_{1/2}$, respectively. After curve fitting, two additional peaks located at 456.0 and 461.8 eV ascribed to $Ti^{3+}2p_{3/2}$ and $Ti^{3+}2p_{1/2}$ peaks could be identified, suggesting the presence of Ti^{3+} species[14] [Fig. 3(a)]. The O1s core level spectrum is asymmetric; besides the main peak of O1s located at 530.1eV a shoulder peak at higher binding energies located at 532.4 eV can be identified after curve fitting, corresponding to chemisorbed H_2O molecules on the sample surface [Fig. 3(b)]. This also indicates the existence of oxygen vacancy sites or Ti^{3+} defect sites on the sample surface.[15–17] For the non-irradiated sample, no additional peaks except for those of $Ti^{4+}2p_{3/2}$ and $Ti^{4+}2p_{1/2}$ could be identified in its core level spectra of Ti2p [Fig. 3(c)]. The shoulder peak at 531.5 eV in the O1s core level spectra [Fig. 3(d)] can be assigned to physisorbed H_2O molecules on the sample. It can be concluded that UV light can induce the formation of oxgen vacancy defects on the sample surfaces.

The structure of the TiO_2 sample calcined at 100 °C was further studied by electron diffraction. The SAED pattern (Fig. 4) of the sample shows a seriously defective area, indicating the existence of defects in the sample. The observed diffraction pattern can be indexed as a tetragonal phase along [100] direction. Moreover, streaks along [110] direction reveal the existence of planar defects in the sample.[18,19]

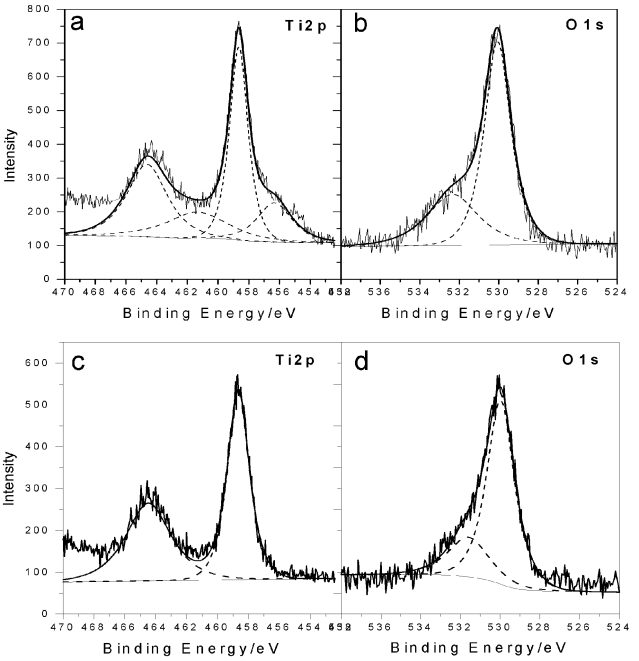

Fig. 3 The Ti2p and O1s core level spectra of the UV-irradiated sample (a,b) and non-irradiated sample (c,d) annealed at 100 °C. Dashed lines show the curve fitting results.

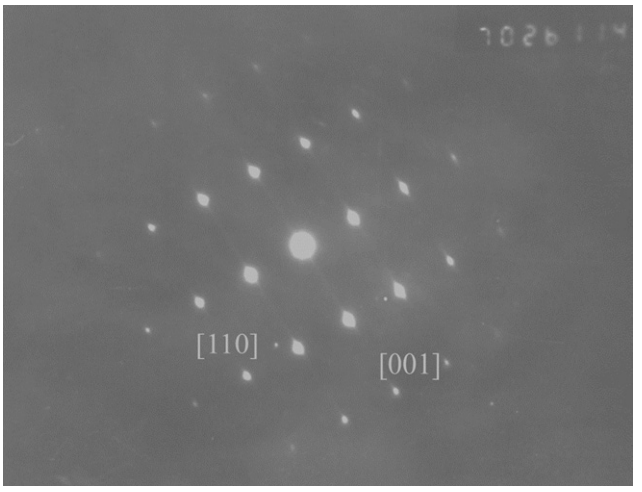

Fig. 4 The selected area electron diffraction (SAED) pattern of a 100 °C annealed sample. The diffraction spots and streaks imply that the sample contains single crystal and planar defects.

The ultraviolet light introduced during the TiO_2 colloid preparation can generate oxygen vacancy defects in the colloid, just as ultraviolet illumination may create surface oxygen vacancies on TiO_2 thin films.[17,20] These vacancies can act as nucleation sites to promote the transition from amorphous to anatase at low calcination temperatures. On the other hand, since the transition involves an overall contraction or shrinking of the oxygen framework, as indicated by a volume shrinkage of approximately 8%, and a cooperative movement of ions, the removal of oxygen ions might be expected to accelerate the transition from amorphous to anatase.

In summary, phase-pure anatase with high crystallinity and small particle size was synthesized at relatively low temperature by using a photo-assisted sol-gel method. Experimental

results indicate that the formation of anatase phase can be promoted by oxygen deficiencies induced by UV irradiation during the sol-gel process. We expect that such a photo-assisted sol-gel methodology can be applied to the preparation of other semiconductor oxides with small particle size and high crystallinity at low annealing temperatures.

Experimental

TiO_2 colloids were prepared by using the standard sol-gel method except photo-irradiation was applied. A dry 2-propanol solution (10.5 ml) containing 5.4 ml of titanium(IV) isopropoxide {Ti $[OCH(CH_3)_2]_4$, Acros, $>98\%$} was slowly added into a 30 ml alcohol solution containing 2.5 ml hydrochloric acid and 1.0 ml deionized water under vigorous stirring. During the experiment the Pyrex reactor that transmits light with wavelengths longer than 290 nm was illuminated for about 8 h by a 500 W high-pressure mercury lamp; a 1.0 cm thick circulating water cuvette is used to avoid thermal heating by the lamp. The distance between the lamp and reactor was 15 cm and the intensity of the UV radiation reaching the reactor was measured to be about 20 mW cm^{-2} by a radiometer. The powder samples were prepared by evaporating the solvent from the colloids and then annealing the TiO_2 gels at different temperatures. Control experimental data were also collected, using the identical sol-gel method except that no photo-irradiation was performed.

The powder X-ray diffraction patterns were collected with Cu Kα radiation ($\lambda = 1.5406$ Å) at a scan rate of 0.02° per 0.12 s. The average grain size was calculated based on the Scherrer formula. Raman spectra were taken on a Renishaw-2000 Raman spectrometer at resolution of 2 cm^{-1} by using the 514.5 nm line of an Ar ion laser as the excitation source. The BET surface area of the samples, which had been degassed at 300 K for 3–4 h, was measured by the adsorption of N_2 molecules at 77 K. XPS (X-ray photoelectron spectroscopy) measurements were carried out with an ESCA Lab 220i-XL spectrometer by using a unmonochromated Al Kα (1486.6 eV) X-ray source. All the spectra were calibrated to the binding energy of the adventitious C1s peak at 284.6 eV. For TEM (SAED) observations, the powdered samples were dispersed in ethanol and then deposited onto carbon-coated copper grids. After solvent evaporation, the samples were observed with a JEM-200CX electron microscope at an accelerating voltage of 200 kV.

Acknowledgements

This work was supported by National Science Foundation of China, Chinese Academy of Sciences and National Research Fund for Fundamental Key Projects No.973 (G19990330).

References

1 E. Pelizzetti, C. Minero, E. Borgarello, L. Tinucci and N. Serpone, *Langmuir*, 1993, **9**, 2995.
2 A. Hattori, M. Yamamoto, H. Tada and S. Ito, *Chem. Lett.*, 1998, **8**, 707.
3 M. A. Fox and M. T. Dulay, *Chem. Rev.*, 1993, **93**, 341.
4 I. Sopyan, S. Murasawa, K. Hashimoto and A. Fujishima, *Chem. Lett.*, 1998, **10**, 723.
5 Z. Zhang, C. C. Wang, R. Zakaria and J. Y. Ying, *J. Phys. Chem B*, 1998, **102**, 10 871.
6 E. A. Barringer and H. K. Bowen, *J. Am. Ceram. Soc.*, 1982, **65**, C199.
7 Z. S. Guan, X. T. Zhang, Y. Ma, Y. A. Cao and J. N. Yao, *J. Mater. Res.*, 2001, **16**, 907.
8 G. A. Tompsett, G. A. Bowmaker and T. P. Cooney, *J. Raman Spectrosc.*, 1995, **26**, 57.
9 U. Balachandran and N. G. Eror, *J. Solid. State. Chem.*, 1982, **42**, 276.
10 P. P. Ahonen, E. I. Kauppinen, J. C. Joubert, J. L. Deschanvres and G. Van Tendeloo, *J. Mater. Res.*, 1999, **14**, 3938.
11 J. C. Parker and R. W. Siegel, *Appl. Phys. Lett.*, 1990, **57**, 943.
12 J. C. Parker and R. W. Siegel, *J. Mater. Res.*, 1990, **5**, 1246.
13 E. H. Poniatowski and R. R. Talavera, *J. Mater. Res.*, 1994, **9**, 2102.
14 A. N. Shultz, W. Jang, W. M. Hetherington, D. R. Baer, L. Q. Wang and M. H. Engelhard, *Surf. Sci.*, 1995, **339**, 114.
15 W. Göpel, J. A. Anderson, D. Frankel, M. Jaehnig, K. Phillips, J. A. Schafer and G. Rocker, *Surf. Sci.*, 1984, **139**, 333.
16 R. L. Kurtz, R. Stockbauer, T. E. Madey, E. Roman and J. L. Desegovia, *Surf. Sci.*, 1989, **218**, 178.
17 N. Sakai, R. Wang, A. Fujishima, T. Watanabe and K. Hashimoto, *Langmuir*, 1998, **14**, 5918.
18 J. S. Anderson and R. J. D. Tilley, *J. Solid State Chem.*, 1970, **2**, 472.
19 Z. Q. Li, S. Ramasamy, H. Hahn and R. W. Siegel, *Mater. Lett.*, 1988, **6**, 195.
20 R. Wang, K. Hashimoto, A. Fujishima, M. Chikuni, E. Kojima, A. Kitamara, M. Shimohigshi and T. Watanabe, *Adv. Mater.*, 1998, **10**, 135.